A STATE SPACE APPROACH TO NOISE REDUCTION OF 3D FLUORESCENT MICROSCOPY IMAGES

Raimund J. Ober[1,4], *Xuming Lai*[1,2,3], *Zhiping Lin*[2*], *E. Sally Ward*[3,4]

[1]Department of Electrical Engineering, University of Texas at Dallas, Richardson, TX, 75083, USA.
[2]School of Electrical and Electronic Engineering, Nanyang Technological University, Block S2, Nanyang Avenue, Singapore 639798, Republic of Singapore.
[3]Center for Immunology, University of Texas Southwestern Medical Center, Dallas, TX, 75390, USA.
[4]Cancer Immunobiology Center, University of Texas Southwestern Medical Center, Dallas, TX, 75390, USA.

ABSTRACT

An algorithm is presented to calculate a state space realization of a 3D image set. It is based on interpreting the image set as the impulse response of a 3D separable system. As an application it is shown how the approximation steps, including balanced model reduction methods, in the algorithm can be used to suppress noise in 3D image sets. The approach was motivated by a practical problem in the analysis of 3D fluorescent microscopy image data of fluorescently labelled cells.

1. INTRODUCTION

Noise suppression is an important aspect in the analysis of 3D fluorescent microscopy image sets. The signal levels of fluorescent microscopy images are typically very low even when highly sensitive detectors are used [1]. In addition, the signal, i.e. the photons emitted by the fluorescent tags, is itself a random process. There are also various noise sources in the system ranging from scattered photons to readout noise in the CCD camera [1]. This means that the images have low signal to noise ratios. As a result, noise becomes a serious obstacle to the use of such acquired images in many image processing algorithms, i.e. deconvolution algorithms (see e.g. [2]). As a standard method, a Gaussian filter is often used to smooth 3D image sets [3]. However, since the Gaussian filtering approach is based on a weighted average of neighboring pixels, it typically results in the loss of sharp details in 3D image sets. It is therefore desirable to develop alternative methods for noise reduction of 3D fluorescent microscopy images.

Many advanced signal processing techniques call for the use of state space models. The question arises whether it

is possible to also obtain a state space representation for a 3D image set and address the noise reduction problem at the same time. An affirmative answer is provided in this paper. State space realizations have been used for multidimensional filter design (see [4] and the references therein). One of the most suitable forms of realizations is balanced state space realization, since it can be easily used in balanced model reduction, which has several desirable properties such as an error bound and preservation of the stability of the original system (see e.g. [5]). In addition, state space realizations were also used together with singular value decomposition to design a 2D separable-denominator digital filter (see e.g. [6]).

In this paper we present a new algorithm to calculate a state space realization of a 3D image set by considering the image set as the impulse response of a 3D separable system. When noise is presented in 3D image sets, the algorithm is capable of reducing noise components and obtaining smoothed estimates of image sets.

2. METHODS

Our algorithm can be separated into two parts. In the first part of the algorithm (Algorithm 1) a non-iterative method is introduced to decompose a 3D image set to three cascaded 1D components via singular value decompositions. Though singular value decompositions were used in the low-rank approximation of a 3D array [7]. The algorithm given in [7] is an iterative algorithm and computationally very intense. In the second part of the algorithm (Algorithm 2) the balanced realizations of the one-dimensional components are calculated via the modified Kung's algorithm [8].

2.1. Decomposition of a three-dimensional image set

Algorithm 1 *Let $P(k_1, k_2, k_3)$, $k_i = 1, 2, \ldots, N_i$, $i = 1, 2, 3$, represent a three-dimensional image set.*

1. *Arrange the entries of P in a matrix Q_3 as*

$$Q_3 = \begin{bmatrix} P(1,1,1) & P(1,1,2) & \cdots \\ P(2,1,1) & P(2,1,2) & \cdots \\ P(3,1,1) & P(3,1,2) & \cdots \\ \vdots & \vdots & \\ P(N_1,1,1) & P(N_1,1,2) & \cdots \end{bmatrix}$$

$$\begin{matrix} \cdots & P(1,2,1) & \cdots & P(1,N_2,N_3) \\ \cdots & P(2,2,1) & \cdots & P(2,N_2,N_3) \\ \cdots & P(3,2,1) & \cdots & P(3,N_2,N_3) \\ \vdots & \vdots & & \vdots \\ \cdots & P(N_1,3,1) & \cdots & P(N_1,N_2,N_3) \end{matrix} \Bigg],$$

where $Q_3 \in \mathbb{R}^{N_1 \times N_2 N_3}$.

2. *Decompose Q_3 via the singular value decomposition as $Q_3 = U_1 \Sigma_1^{1/2} \Sigma_1^{1/2} V_1$.*

3. *Partition $\Sigma_1 = diag(\hat{\Sigma}_1, \check{\Sigma}_1)$, $U_1 = [\hat{U}_1, \check{U}_1]$, and $V_1 = \begin{bmatrix} \hat{V}_1 \\ \check{V}_1 \end{bmatrix}$ conformally, where $\hat{\Sigma}_1 \in \mathbb{R}^{l_1 \times l_1}$, $\check{\Sigma}_1 \in \mathbb{R}^{r_1 \times r_1}$, $\hat{U}_1 \in \mathbb{R}^{N_1 \times l_1}$, $\check{U}_1 \in \mathbb{R}^{N_1 \times r_1}$, $\hat{V}_1 \in \mathbb{R}^{l_1 \times N_2 N_3}$, and $\check{V}_1 \in \mathbb{R}^{r_1 \times N_2 N_3}$. Let $L_3^{r_1} := \hat{U}_1 \hat{\Sigma}_1^{1/2}$, and $R_3^{r_1} := [R_3^{r_1}(1), \ldots, R_3^{r_1}(N_2 N_3)] := \hat{\Sigma}_1^{1/2} \hat{V}_1$, where $R_3^{r_1}(i) \in \mathbb{R}^{l_1 \times l}$, $i = 1, 2, \ldots, N_2 N_3$. Then $Q_3 \approx \hat{Q}_3^{r_1} := L_3^{r_1} R_3^{r_1}$ is an approximate factorization, where r_1 denotes the dropped singular values. The factorization is exact for $r_1 = 0$, i.e. $Q_3 = \hat{Q}_3^0 = L_3^0 R_3^0$. Let*

$$P_1^{r_1} := \begin{bmatrix} P_1^{r_1}(1) \\ P_1^{r_1}(2) \\ P_1^{r_1}(3) \\ \vdots \\ P_1^{r_1}(N_1) \end{bmatrix} := L_3^{r_1}, \text{ where } P_1^{r_1}(k_1) \in$$

$\mathbb{R}^{1 \times l_1}$, $k_1 = 1, 2, \ldots, N_1$.

4. *Rearrange the elements of $R_3^{r_1}$ to form Q_2 as*

$$Q_2 := \begin{bmatrix} R_3^{r_1}(1) & \cdots & R_3^{r_1}(N_3) \\ R_3^{r_1}(N_3+1) & \cdots & R_3^{r_1}(2N_3) \\ R_3^{r_1}(2N_3+1) & \cdots & R_3^{r_1}(3N_3) \\ \vdots & \vdots & \vdots \\ R_3^{r_1}((N_2-1)N_3+1) & \cdots & R_3^{r_1}(N_2 N_3) \end{bmatrix}.$$

5. *Decompose Q_2 via the singular value decomposition as $Q_2 = U_2 \Sigma_2^{1/2} \Sigma_2^{1/2} V_2$.*

6. *Partition $\Sigma_2 = diag(\hat{\Sigma}_2, \check{\Sigma}_2)$, $U_2 = [\hat{U}_2, \check{U}_2]$, and $V_2 = \begin{bmatrix} \hat{V}_2 \\ \check{V}_2 \end{bmatrix}$ conformally, where $\hat{\Sigma}_2 \in \mathbb{R}^{l_2 \times l_2}$, $\check{\Sigma}_2 \in \mathbb{R}^{r_2 \times r_2}$, $\hat{U}_2 \in \mathbb{R}^{N_2 l_1 \times l_2}$, $\check{U}_2 \in \mathbb{R}^{N_2 l_1 \times r_2}$, $\hat{V}_2 \in \mathbb{R}^{l_2 \times N_3}$, and $\hat{V}_2 \in \mathbb{R}^{r_2 \times N_3}$. Let $L_2^{r_2} := \hat{U}_2 \hat{\Sigma}_2^{1/2}$, and $R_2^{r_2} := \hat{\Sigma}_2^{1/2} \hat{V}_2$. Then $Q_2 \approx \hat{Q}_2^{r_2} := L_2^{r_2} R_2^{r_2}$ is an approximate factorization. The factorization is exact for $r_2 = 0$, i.e. $Q_2 = \hat{Q}_3^0 = L_2^0 R_2^0$. Let $P_2^{r_2} :=$*

$$\begin{bmatrix} P_2^{r_2}(1) \\ P_2^{r_2}(2) \\ P_2^{r_2}(3) \\ \vdots \\ P_2^{r_2}(N_2) \end{bmatrix} :=$$

$L_2^{r_2}$ and $P_3^{r_2} := [P_3^{r_2}(1), P_3^{r_2}(2), \ldots, P_3^{r_2}(N_3)] := R_2^{r_2}$, where $P_2^{r_2}(k_2) \in \mathbb{R}^{l_1 \times l_2}$, $k_2 = 1, 2, \ldots, N_2$, and $P_3^{r_2}(k_3) \in \mathbb{R}^{l_2 \times 1}$, $k_3 = 1, 2, \ldots, N_3$.

In this algorithm an approximate decomposition of the image data points was obtained

$$P(k_1, k_2, k_3) \approx P^{r_1, r_2}(k_1, k_2, k_3) := P_1^{r_1}(k_1) P_2^{r_2}(k_2) P_3^{r_2}(k_3),$$

$k_i = 1, 2, \ldots, N_i$, $i = 1, 2, 3$. If no approximation is carried out, i.e. if $r_1 = r_2 = 0$, we have the exact factorization

$$P(k_1, k_2, k_3) = P^{0,0}(k_1, k_2, k_3) = P_1^0(k_1) P_2^0(k_2) P_3^0(k_3),$$

$k_i = 1, 2, \ldots, N_i$, $i = 1, 2, 3$.

2.2. Balanced state space realizations of finite one-dimensional sequences

Algorithm 2 *Let $P_j(i) \in \mathbb{R}^{p \times m}$, $i = 1, 2, \ldots, N$ and j is an integer, be a finite one-dimensional sequence.*

1. *Construct the $(N+1)p \times (N+1)m$ Hankel matrix*

$$H = \begin{bmatrix} P_j(1) & P_j(2) & \cdots & P_j(N-1) & P_j(N) & 0 \\ P_j(2) & P_j(3) & \cdots & P_j(N) & 0 & 0 \\ \vdots & \vdots & & & \vdots & \vdots \\ P_j(N) & 0 & \cdots & \cdots & 0 & 0 \\ 0 & 0 & \cdots & \cdots & 0 & 0 \end{bmatrix},$$

where 0 denotes a block of zeros of size $p \times m$.

2. *Let $H = U\Sigma V$ be a singular value decomposition.*

3. *Partition $\Sigma = diag(\Sigma_1, \Sigma_2)$, $\Sigma_1 \in \mathbb{R}^{n \times n}$, $\Sigma_2 \in \mathbb{R}^{s \times s}$, $U = [U_1, U_2]$, $U_1 \in \mathbb{R}^{(N+1)p \times n}$, $U_2 \in \mathbb{R}^{(N+1)p \times s}$, and $V = \begin{bmatrix} V_1 \\ V_2 \end{bmatrix}$, $V_1 \in \mathbb{R}^{n \times (N+1)m}$, $V_2 \in \mathbb{R}^{s \times (N+1)m}$, conformally.*

4. *Let $C_j^s \in \mathbb{R}^{p \times n}$ be the first p rows of $U_1 \Sigma_1^{1/2}$.*

5. *Let $B_j^s \in \mathbb{R}^{n \times m}$ be the first m columns of $\Sigma_1^{1/2} V_1$.*

6. Let $U_1 = \begin{bmatrix} \bar{U}^1_{11} \\ \vdots \\ \bar{U}^1_{N1} \\ \bar{U}^1_{(N+1)1} \end{bmatrix}$, where $\bar{U}^1_{t_11} \in \mathbb{R}^{p \times n}$ for all

$t_1 = 1, \ldots, N+1$, and define $U^\uparrow_1 = \begin{bmatrix} \bar{U}^1_{21} \\ \vdots \\ \bar{U}^1_{(N+1)1} \end{bmatrix}$

and $U^\downarrow_1 = \begin{bmatrix} \bar{U}^1_{11} \\ \vdots \\ \bar{U}^1_{N1} \end{bmatrix}$. Then let $A^s_j = \Sigma_1^{-1/2} U_1^{\downarrow *} U_1^\uparrow \Sigma_1^{1/2} \in$

$\mathbb{R}^{n \times n}$.

Then (A^s_j, B^s_j, C^s_j) is called a state space realization of P_j, i.e. $P(i) \approx C^s_j (A^s_j)^{i-1} B^s_j$, $i = 1, 2, \ldots, N$. If no singular values are dropped, i.e. $s = 0$, we obtain an exact realization. For more details and properties of the above state space realization, see [9].

2.3. State space realizations of a 3D image set

Let $P(k_1, k_2, k_3), k_i = 1, 2, \ldots, N_i$, $i = 1, 2, 3$, be a 3D image set. We decompose the image set and obtain three 1D sequences $P_1^{r_1}, P_2^{r_2}$ and $P_3^{r_2}$ via Algorithm 1 with some parameters $r_1 \geq 0$ and $r_2 \geq 0$. For each 1D component with appropriately chosen reduction parameters s_1, s_2, and s_3 approximate realizations $(A_1^{r_1;s_1}, B_1^{r_1;s_1}, C_1^{r_1;s_1})$, $(A_2^{r_2;s_2}, B_2^{r_2;s_2}, C_2^{r_2;s_2})$ and $(A_3^{r_2;s_3}, B_3^{r_2;s_3}, C_3^{r_2;s_3})$ are derived using Algorithm 2. Note that r_1, r_2 denote the numbers of the dropped singular values in the two singular value decompositions used to decompose the image set P in Algorithm 1 and s_1, s_2, s_3 are the numbers of the discarded singular values in the other three singular value decompositions used to calculate the realizations in Algorithm 2. The smoothed estimate of the 3D image set P obtained is then denoted as $P^{r_1,r_2;s_1,s_2,s_3}$ and we have

$$\begin{aligned} P(k_1, k_2, k_3) &\approx P^{r_1,r_2;s_1,s_2,s_3}(k_1, k_2, k_3) \\ &:= P_1^{r_1;s_1}(k_1) \times P_2^{r_2;s_2}(k_2) \times P_3^{r_2;s_3}(k_3) \\ &:= C_1^{r_1;s_1}(A_1^{r_1;s_1})^{k_1-1} B_1^{r_1;s_1} \\ &\quad \times C_2^{r_2;s_2}(A_2^{r_2;s_2})^{k_2-1} B_2^{r_2;s_2} \\ &\quad \times C_3^{r_2;s_3}(A_3^{r_2;s_3})^{k_3-1} B_3^{r_2;s_3}, \end{aligned}$$

where $k_i = 1, 2, \ldots, N_i$, $i = 1, 2, 3$. If in neither of the two algorithms approximations are carried out we have an exact realization of the image set given by $P(k_1, k_2, k_3) = P^{0,0;0,0,0}(k_1, k_2, k_3)$.

Note that the actual performance of the approximation algorithm is in general not independent of the particular assignment of which spatial dimension corresponds to which index in the image array P, in part due to the different sizes of the three 1D components. We have found, for example,

for microscopy image data it is often advisable that the middle index k_2 corresponds to the optical axis, if fewer data points are available in this direction than in the others.

### 3. STATE SPACE REALIZATIONS OF BIOMEDICAL IMAGES AND NOISE REDUCTION

We apply our algorithm to a 3D fluorescent microscopy image set P of a mouse T cell. The T cell receptor has been labeled with fluorescent tags and is therefore visible by fluorescent microscopy. All images of this 3D image set and two sample cross sections are shown in Figure 1.

We first apply our algorithm to the 3D image set without carrying out approximations. Based on the notation introduced in Methods section, the estimated image set is denoted as $P^{0,0;0,0,0}$. Figure 2.a1 show a cross section of $P^{0,0;0,0,0}$. The root-mean-square error (RMSE) between the estimated image set and the original image set is 7.4×10^{-10} for the scale used for displays. This shows that up to insignificant numerical errors an exact state space realization was obtained. It is interesting to note that the significant background intensity level has also been accurately matched by the realization algorithm.

To suppress noise of the image set P we use our algorithm to obtain a realization of the image set with approximations. As discussed in Methods section, the approximation is essentially based on splitting the set of singular values of each singular value decomposition in two subsets. One, typically the larger ones, that will be 'retained' and two, typically the smaller ones, that will be 'discarded' to provide the approximation. Due to the presence of noise in the image set, small singular values are corrupted by noise. By excluding those singular values, we effectively suppress noise and obtain a smoothed approximation of the noisy image set.

In this case, we choose to retain 15 and 30 singular values in the first two singular values decompositions used to decompose the image set P and keep 60, 300 and 100 singular values in the other three singular value decompositions when calculating the realizations. Due to the limitation of space, we do not explain how to obtain these numbers here, which can be found in a related paper on noise suppression of point spread functions [10]. The total number of non-zero singular values for the five singular value decomposition is 99, 110, 99, 315 and 110. Therefore, we dropped 84, 80, 39, 15 and 10 singular values respectively. From the notations introduced in Methods section, the smoothed estimate of the image set P is denoted as $P^{84,80;39,15,10}$. Figure 2.a2 show the cross section of the image set $P^{84,80;39,15,10}$. The difference between the smoothed image frame and the original image frame, shown in Figure 2.a5 appears as random noise and no significant error is introduced. For comparison, we also applied a Gaussian filter of size 3*3*3 with standard

1155

deviation of one in all directions to the 3D image set. The resultant image for the corresponding image frame is shown in 2.a3 and the difference between the smoothed image set and the original image set is shown in Figure 2.a6. As can be seen, the error by the Gaussian filter method is bigger than that using our method.

(a)   (b)
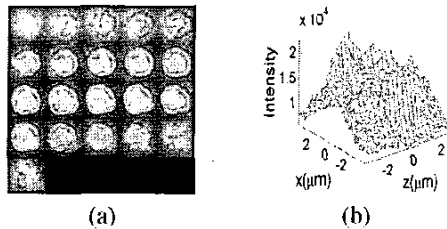
Fig. 1. (a) All two-dimensional images of a three-dimensional fluorescent microscopy image set of a T cell. The image series was acquired on a Zeiss inverted microscope with a 100x Plan-Aprochromat NA 1.4 objective using a high sensitivity Hamamatsu Orca 100 Peltier cooled 12 bit CCD camera. The image set consists of 21 images each being a 99×110 pixel array. The images are assumed to be $300nm$ apart. Each pixel is assumed to be $67nm \times 67nm$ in size. Therefore, Each frame has a size of $6.633\mu m \times 7.37\mu m$. The panel is arranged such that the frames are displayed sequentially from left to right and top to bottom. (b) is the cross section $P(60, k_2, k_3)$, $k_2 = 1, \ldots, 21$, $k_3 = 1, \ldots, 110$ of the image set.

4. REFERENCES

[1] S. Inoue and K. R. Spring, *Video Microscopy: The Fundamentals*, Plenum Pub Corp., 1997.

[2] G. M. P. van Kempen, L. J. van Vliet, P. J. Verveer, and H. T. M. van der Voort, "A quantitative comparison of image restoration methods for confocal microscopy," *Journal of Microscopy*, vol. 185, pp. 354–365, 1997.

[3] G. M. P. van Kempen and L. J. van Vliet, "Improving the restoration of textured objects with prefiltering," in *Proceeding of 3rd Annual Conference of the Advanced School for Computing and Imaging (ASCI'97)*, 1997, pp. 174–179.

[4] A. Doi and T. Hinamoto, "A spatial-domain technique for the design of 3-D separable-denominator state-space digital filters," *Multidimensional Systems and Signal Processing*, vol. 12, pp. 89–98, 2001.

[5] K. Zhou, J. C. Doyle, and K. Glover, *Robust Optimal Control*, Prentice-Hall, Inc., New Jersey, 1996.

(a1)   (a2)   (a3)

(a4)   (a5)   (a6)
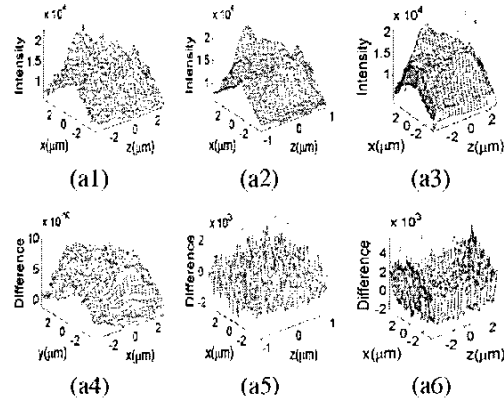
Fig. 2. Comparison of the exact estimate of $P^{0,0;0,0,0}$, the approximated estimate $P^{84,80;39,15,10}$ of the image set P obtained via our algorithm, and the Gaussian filter method. (a1),(a2),(a4),(a5) show the cross section $P^{0,0;0,0,0}(60, k_2, k_3)$, $k_2 = 1, \ldots, 21$, $k_3 = 1, \ldots, 110$, the corresponding cross section of $P^{84,80;39,15,10}$, and the difference between them and the corresponding cross section of P (Figure 1.b) in the X-Z plane. (a3),(a6) show the cross section and the difference image by the Gaussian filter.

[6] T. Lin, M. Kawamata, and T. Higuchi, "Design of 2-D separable-denominator digital filters based on the reduced-demensional decomposition," *IEEE Transactions on Circuits and Systems*, vol. CAS-34, no. 8, pp. 934–941, 1987.

[7] W. S. Lu and S. C. Pei, "On optimal low-rank approximation of multidimensional discrete signals," *IEEE Transactioins on Circuits and Systems-II*, vol. 45, no. 3, 1998.

[8] S. Y. Kung, "A new identification and model reduction algorithm via singular value decompositions," in *Proceeding 12th Asilomar Conference on Signals, Systems and Computers*, 1978, pp. 705–714.

[9] R. J. Ober, X. Lai, Z. Lin, and E. S. Ward, "State space realization of a three-dimensional image set with application to noise reducion of fluorescent microscopy images of cells," *To appear in Multidimensional Systems and Signal Processing*, 2004.

[10] X. Lai, Z. Lin, E. S. Ward, and R. J. Ober, "Noise suppression of point spread functions and its influence on deconvolution of three-dimensional fluorescence microscopy image sets," *submitted to Journal of Microscopy (revised)*, 2003.